Analysis on Discharge Modes in AC Plasma Display Panel With Sustain Gap of 200 μm

Jae Young Kim and Heung-Sik Tae, *Senior Member, IEEE*

***Abstract*—The V_t close-curve measurement shows that there exists a surface (X–Y) discharge contour in spite of a large sustain gap of 200 μm greater than a barrier rib height of 125 μm. This indicates that there are two different discharge modes, i.e., one mode is to produce the surface discharge, and the other is to produce the surface discharge including the plate gap discharge. The two discharge modes are examined and analyzed based on the V_t close-curve movement on the cell voltage plane. The two discharge modes show the different discharge characteristics such as the sustain voltage level, V_t close-curve behavior, luminance, and luminous efficiency. In addition, the spatial wall charge, electron density behaviors, and their current flows as a function of time are investigated in detail using the numerical analysis.**

***Index Terms*—Alternating current plasma display panel (ac-PDP), different discharge modes, large sustain gap, V_t close curve.**

I. Introduction

OVER THE PAST few years, a considerable number of studies have been tried to improve the luminous efficiency of an ac plasma display panel (ac-PDP) [1], [2]. In the ac-PDP using the microdischarge within a small discharge volume, efforts to improve the luminous efficiency by extending the discharge path have been tried [3]–[7]. In a conventional PDP cell with a sustain gap of about 60–80 μm, the sustain discharge is directly initiated between two sustain electrodes because the sustain gap distance is shorter than the barrier rib height of about 120 μm. However, in a PDP cell with a large sustain gap of 400 μm greater than the barrier rib height of about 120 μm, the discharge should be initially produced between the sustain and address electrodes under an MgO cathode condition, and then the subsequent main discharge should be sustained between the two sustain electrodes [3], [7]. These different discharge paths are possible due to the difference in the relative distances among the three electrodes under the current PDP cell structure with three electrodes. If the sustain gap is about 200 μm under the barrier rib height of about 120 μm, two different discharge modes can be produced in the same cell structure depending on the sustain driving waveforms, i.e., one mode is to produce the surface discharge, and the other is to produce the surface discharge including the plate gap discharge. Such a different discharge path causes the different discharge characteristics, such as luminance, luminous efficiency, discharge current, and wall charge distribution.

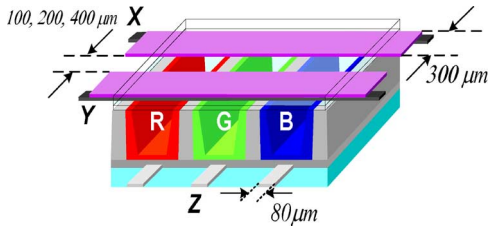

Fig. 1. Discharge cell structure with various sustain electrode gaps such as 100, 200, and 400 μm employed in this paper.

In this paper, two different discharge modes are examined in the cell structure with a sustain gap of 200 μm by adjusting the driving waveforms applied to the three electrodes. The two discharge characteristics are investigated by using the V_t close-curve analysis. The corresponding IR profile, luminance, and luminous efficiency are also examined. Furthermore, the discharge behavior for two different discharge modes, such as the spatial wall charge behavior, the spatial electron density behavior, and their current flows as a function of time, is also numerically examined.

II. Various Sustain Gaps and Related Discharge Modes

The firing voltage conditions among the three electrodes strongly depend on the dimension of the cell structure, especially the variation in a coplanar sustain gap under a constant barrier rib height. Fig. 1 shows the discharge cell structure with various sustain electrode gaps (100, 200, and 400 μm) employed in this paper. The various sustain electrode gaps (100, 200, and 400 μm) are fabricated in the same test panel for more accurately measuring the V_t close curve. The detailed specifications of the 7-in test panel are listed in Table I.

Fig. 2 shows the V_t close curves [8]–[11] with no initial wall charges as a variation in the sustain electrode gap measured from the test panel. Fig. 3(a) shows the initializing waveform for measuring the V_t close curves with no initial wall charge. First, the ramp-type waveform was applied to erase the wall charge that was accumulated by the detecting pulse, and the subsequent square-type waveform with high voltage difference ($\geq$440 V) between the X–Y electrodes was applied to produce the strong discharge, thus resulting in completely eliminating

Manuscript received March 19, 2007; revised July 17, 2007. This work was supported by Brain Korea 21 (BK21).

The authors are with the School of Electrical Engineering and Computer Science, Kyungpook National University, Daegu 702-701, Korea (e-mail: hstae@ee.knu.ac.kr).

Color versions of one or more of the figures in this paper are available online at http://ieeexplore.ieee.org.

Digital Object Identifier 10.1109/TPS.2007.910689

TABLE I
SPECIFICATIONS OF THE 7-in TEST PANEL

Front Panel		Rear Panel	
ITO width	300 μm	Barrier rib width	55 μm
Sustain gaps	100, 200, 400 μm	Barrier rib height	125 μm
		Address width	80 μm
Bus width	50 μm	Red phosphor	$(Y,Gd)BO_3$:Eu
Dielectric	30 μm	Green phosphor	$(Zn,Mn)_2SIO_4$
MgO	5000 Å	Blue phosphor	$(Ba,Eu)MgAl_{10}O_{17}$
Gas chemistry	Ne-Xe (5 %)		
Barrier rib	Stripe rib		
Pressure	500 Torr		

the wall charges by inducing the ensuing strong self-erasing discharge. The IR emission was monitored to check whether the self-erasing discharge was produced. In addition, to exclude the priming effect, the detecting pulse with a ramp type was applied after 200 μs from an application of the erase pulse. The complete removal of the wall charges accumulating on the three electrodes enables the measurement of V_t close curves with no initial wall charges. To verify the initial state, the measured firing voltage between the X–Y and Y–X electrodes or between the Z–X and Z–Y electrodes should be the same. Fig. 3(b) shows the verification procedure of the initial states in the V_t close curves that were measured using the initializing waveform in Fig. 3(a). As shown in (1) and (2) of Fig. 3(b), without initial wall charges, at points a and b, the potential difference between the X–Y and Y–X electrodes would be Vs and $-$Vs, respectively, whereas the potential difference between the Z–Y and Z–X electrodes would be 1/2Vs and $-1/2$Vs, respectively. Accordingly, the firing voltages at points a and b should be the same value of Vs without the initial wall charge because of the surface discharge symmetry under an MgO cathode condition. Similarly, as shown in (3) and (4) of Fig. 3(b), the firing voltages at points c and d should be the same value of Vs without the initial wall charge because of the plate gap discharge symmetry under an MgO cathode condition. Consequently, the same firing voltages measured at points a and b and at points c and d can guarantee the initial state of the measured V_t close curve.

As shown in the V_t close curves of Fig. 2, which were guaranteed by the verification procedure in Fig. 3, the large X–Y threshold voltage contours are observed in a sustain gap of 100 μm. However, the X–Y threshold voltage contours shrink in a sustain gap of 200 μm and finally not observed in a sustain gap of 400 μm. At a sustain gap of 400 μm with no X–Y threshold voltage contours, as shown in Fig. 2(c), the sustain discharge cannot be directly produced between the two sustain electrodes, which means that the X–Y discharge can be indirectly produced only with the help of the Z–Y discharge [7]. The presence of the X–Y threshold voltage contour in a sustain gap of 200 μm implies that the sustain discharge can be directly produced between the two sustain electrodes if the cell voltage between the two sustain electrodes is applied over 300 V, as shown in Fig. 2(b). Furthermore, like a sustain discharge in a sustain gap of 400 μm, the X–Y discharge can be indirectly produced with a help of the Z–Y discharge in the case of a sustain gap of 200 μm.

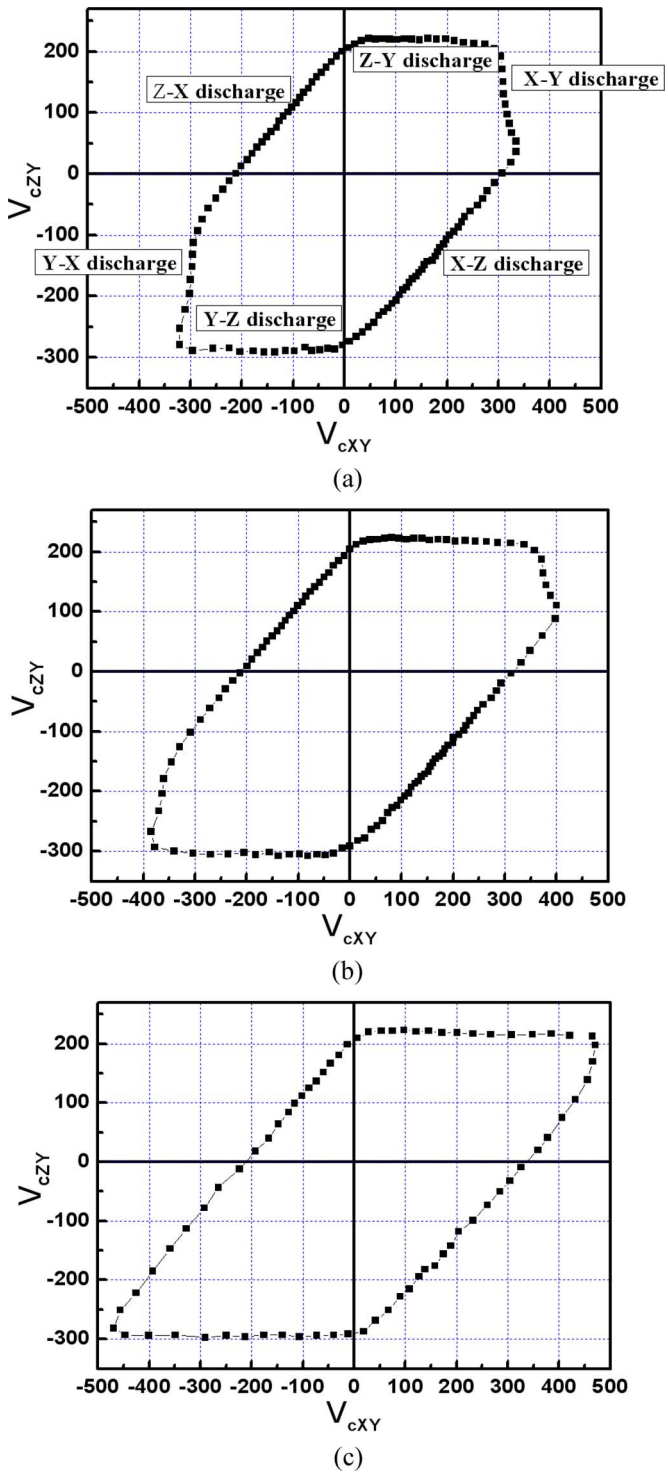

Fig. 2. V_t close curves with no initial wall charges as variations in sustain electrode gap measured from the test panel. (a) 100 μm. (b) 200 μm. (c) 400 μm.

Accordingly, if the proper driving conditions are chosen, two different discharge modes (modes 1 and 2), as shown in Fig. 4, can be produced in a sustain gap of 200 μm. In mode 1 of Fig. 4, the initial discharge is directly produced between the two sustain electrodes when the sustain voltages (V_X and V_Y) are alternately applied to the X and Y electrodes. On the other hand, in mode 2 of Fig. 4, the discharge is initiated between

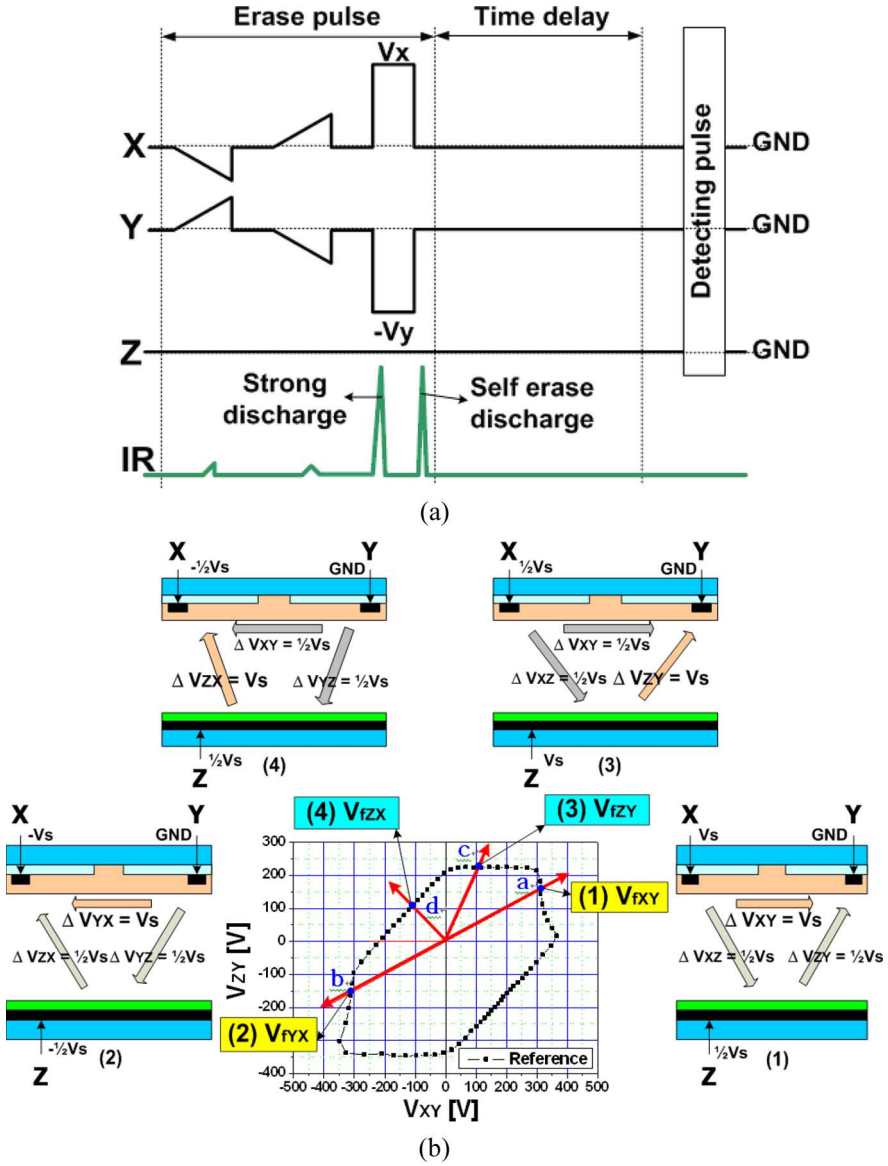

Fig. 3. (a) Initializing waveform for measuring V_t close curves with no initial wall charge. (b) Verification procedure of initial states in V_t close curves measured using the initializing waveform in (a).

the address and sustain electrodes, thus inducing the discharge between the two sustain electrodes when the two voltages (V_X and V_Z) are applied to the X and Z electrodes, respectively. As shown in Fig. 4, in mode 1, the higher sustain voltage (V_X or V_Y) is needed, but in mode 2, the discharge is produced under the low sustain voltage (V_X or V_Y) due to the application of an address voltage (V_Z). The discharge characteristics in two different discharge modes are examined based on a control of the voltage distribution among the three electrodes in a sustain gap of 200 μm.

III. Experimental Results and Discussion

A. Driving Waveforms for Producing Two Different Discharge Modes

Fig. 5(a) and (b) shows the voltage driving waveforms that are applied to the three electrodes so as to produce two different discharge modes (mode 1 and mode 2, respectively). As shown in Fig. 5(a) and (b), instead of the reset and address driving waveforms, the firing voltage waveform is applied to produce the wall charges that are necessary for the sustain discharge voltage. To produce the discharge mode 1 of Fig. 5(a), voltage waveforms (V_X and V_Y) of 300 V are applied to the sustain electrodes X and Y, whereas no voltage waveform V_Z is applied to the address electrode. To produce the discharge mode 2, voltage waveforms (V_X and V_Y) of 190 V are applied to the sustain electrodes X and Y, whereas the voltage waveform (V_Z) of 100 V is applied to the address electrode. For both cases, the driving frequency was 50 kHz, and the width of a sustain pulse ($t_{WX} = t_{WY}$) was 8 μs. The address pulse had a width of 1 μs, and its position coincided with a rising point of the sustain pulse.

Fig. 6 shows the schematic of voltage distribution among the three electrodes in a single cell when the voltage waveforms are applied, as shown in Fig. 5. As shown in (i) of Fig. 6, the firing

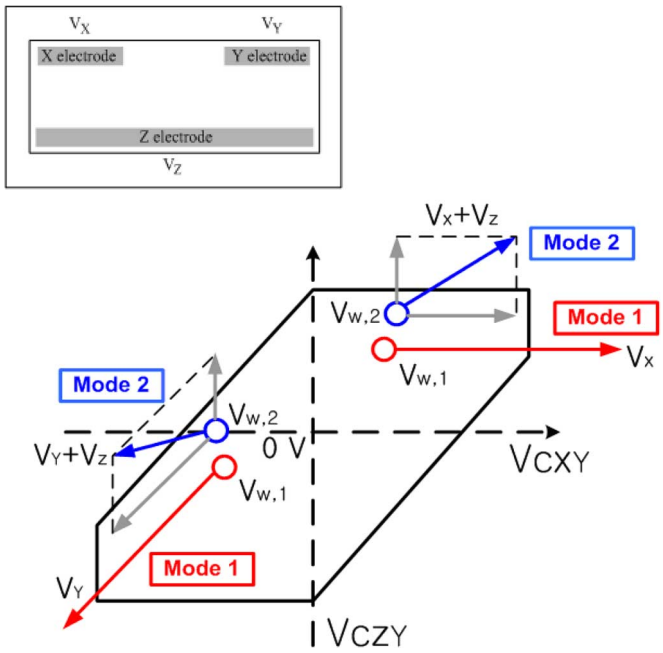

Fig. 4. Two different discharge modes 1 and 2 in the V_t close curve measured from test panel with sustain gap of 200 μm.

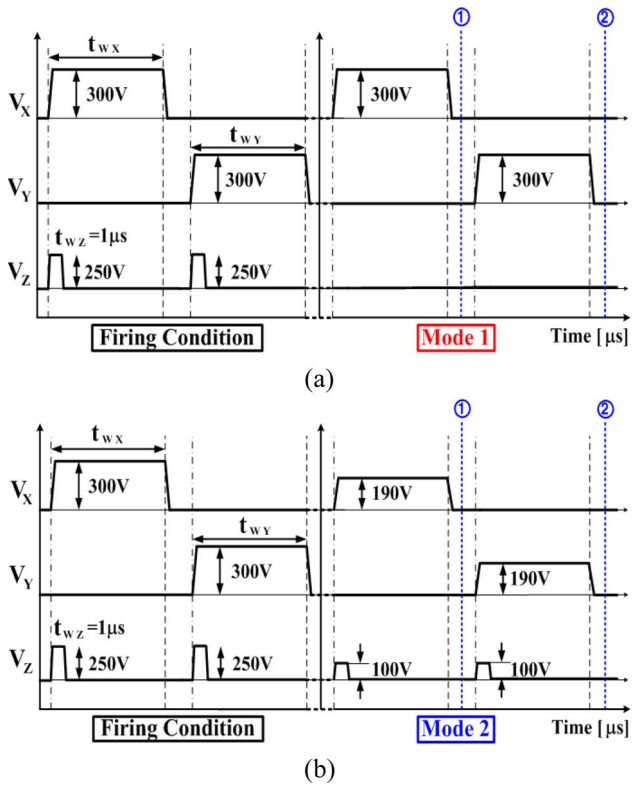

Fig. 5. Voltage waveforms applied to three electrodes in cases of (a) mode 1 and (b) mode 2.

discharge is produced by applying voltages of 300 and 250 V to the sustain (X or Y) and address (Z) electrodes, respectively. After firing the cell, the discharge in mode 1 [in (ii) of Fig. 6] is produced by decreasing only the voltage applied to the address (Z) electrode from 250 to 0 V, whereas the discharge in mode 2 [in (iii) of Fig. 6] is produced by decreasing both the voltages

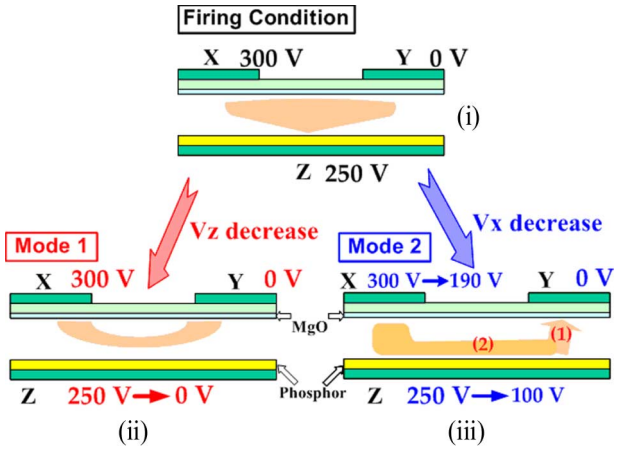

Fig. 6. Two different discharge modes depending on the voltage distributions among the three electrodes, where (ii) mode 1 is produced by only decreasing the voltage on the address electrode from the (i) firing condition, and (iii) mode 2 is produced by decreasing the voltages on both sustain (X) and address (Z) electrodes from the (i) firing condition.

applied to the sustain (X or Y, from 300 to 190 V) and address (Z, from 250 to 100 V) electrodes. The voltage distribution conditions ($V_X = 190$ V, $V_Y = 0$ V, and $V_Z = 100$ V) in mode 2 satisfy the following discharge pathway: prior to the main X–Y discharge, the trigger discharge is initiated between one of the sustain electrodes and the address electrode [process (1) in (iii) of Fig. 6], thus extending toward the other sustain electrode along the address electrode and producing the main discharge [process (2) in (iii) of Fig. 6].

B. V_t Close Curve Measured From Two Different Discharge Modes and Corresponding Wall Charge Behaviors

Fig. 7(a) shows the shrink of the V_t close curves that are measured after the sustain discharge has been produced in discharge mode 1 with respect to the reference V_t close curve. After the discharge between the two sustain electrodes is produced by applying the sustain pulse (V_X) of 300 V to the X electrode, the measured V_t close curve in Fig. 7(b) shows the shrinkage of the V_t close curve instead of the shift of the V_t close curve. In the general case, the shape of the V_t close curve only shifts without deformation if one discharge is produced without additional discharge, such as a self-erasing discharge per one pulse. However, in this case, i.e., in the wide-gap structure, a self-erasing discharge that is additionally produced at a decreasing state of the high sustain pulse of 300 V causes the elimination of some of the wall charges accumulating on the three electrodes. As a result of the wall charge variation induced by the self-erasing discharge, the shape of the V_t close curve shown in Fig. 7(b) was obtained. A detailed description is shown in Fig. 8. Similarly, after the discharge between the two sustain electrodes is produced by applying the sustain pulse (V_Y) of 300 V to the Y electrode, the measured V_t close curve in Fig. 7(c) also shows the shrinkage of the V_t close curve.

Fig. 8(a) shows the schematics of the wall charges that are accumulating on three electrodes during the discharges of mode 1. As shown in Fig. 8(a), the discharge in mode 1 is produced twice, i.e., one discharge is a (i) main discharge when

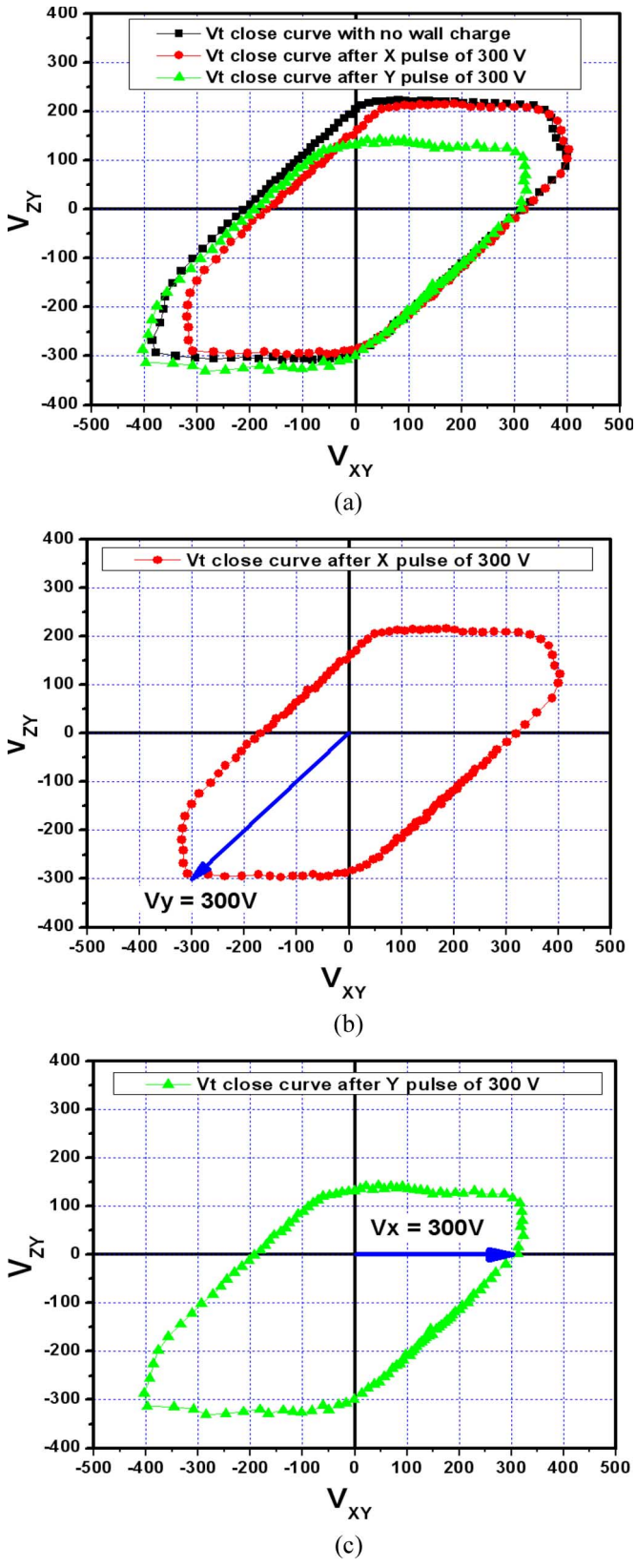

Fig. 7. (a) Shrink of the V_t close curves measured after sustain discharge is produced in discharge mode 1 with respect to the reference V_t close curve. (b) V_t close curve measured after applying the sustain pulse V_X of 300 V to the X electrode. (c) V_t close curve measured after applying the sustain pulse V_Y of 300 V to the Y electrode.

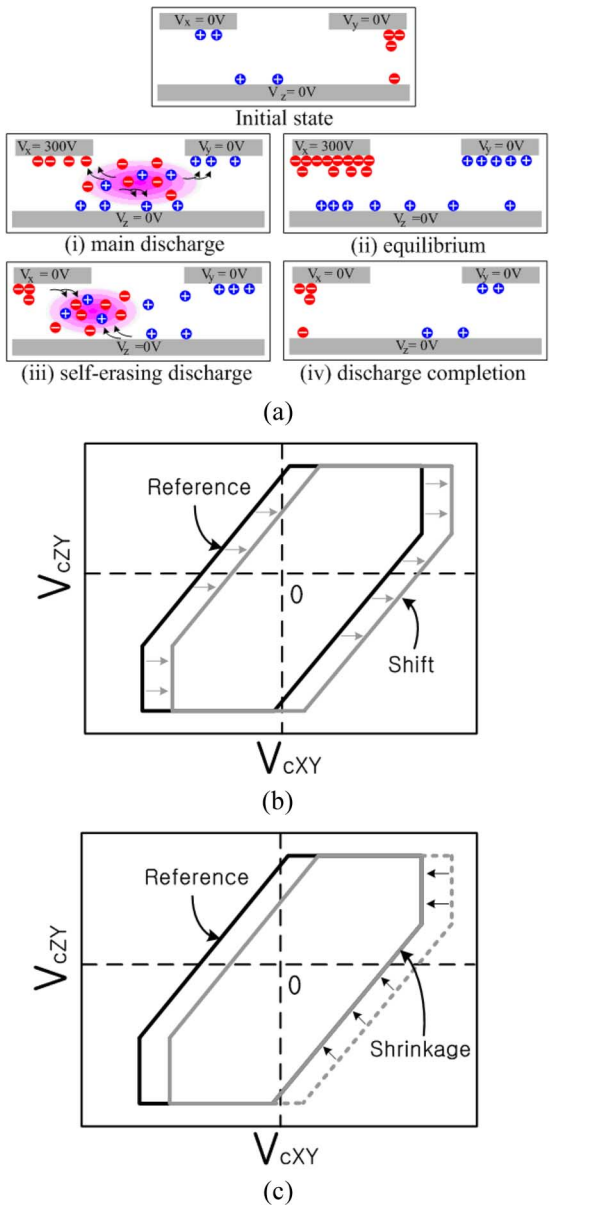

Fig. 8. Schematics of the wall charges accumulating on three electrodes during discharges in (a) mode 1. (b) V_t close curve by wall charges accumulating among the three electrodes after the main discharge. (c) V_t close curve by wall charge variation after self-erasing discharge.

applying a high sustain pulse of 300 V, and the other discharge is a (iii) self-erasing discharge produced only by the wall charges induced by decreasing a high sustain voltage from 300 to 0 V. Since the self-erasing is dominantly produced by the X–Z electrodes because of the wide gap structure, many of the wall charges on the X and Z electrodes are erased, as shown in (iv) of Fig. 8(a). Fig. 8(b) and (c) shows the V_t close curve by wall charges accumulating among the three electrodes after the main discharge and the V_t close curve by the wall charge variation after self-erasing discharge, respectively. Like the conventional case, the wall charges accumulating on the three electrodes shown in (ii) of Fig. 8(a) induce a shift of the V_t close curve with respect to the reference V_t close curve with no initial wall charges, as shown in Fig. 8(b). However, the subsequent self-erasing discharge induces the loss of wall

charges, especially electrons on the X electrode and ions on the Z electrode, as shown in (iii) and (iv) of Fig. 8(a), thereby resulting in the shrinkage of the V_t close curve in both X–Y and X–Z threshold voltage contours in the first and fourth quadrants of the cell voltage plane, as shown in Fig. 8(c).

Unlike the discharge in mode 1, the V_t close curves are shifted with respect to the reference V_t close curve when the discharge in mode 2 is produced, as shown in Fig. 9. After the discharge in mode 2 is produced by applying both the sustain pulse (V_X) of 190 V to the X electrode and the address pulse (V_Z) of 100 V to the address Z electrode, the measured V_t close curve in Fig. 9 shows that the Z–X threshold voltage contour from the first to third quadrant of the cell voltage plane enables the subsequent discharge to be produced by applying both the sustain pulse (V_Y) of 190 V to the Y electrode and the address pulse (V_Z) of 100 V to the address Z electrode. Similarly, as shown in the V_t close curve of Fig. 9(c), which was measured after applying both the sustain pulse (V_Y) of 190 V to the Y electrode and the address pulse (V_Z) of 100 V to the address Z electrode, the Z–Y threshold voltage contour in the first quadrant of the cell voltage plane enables the subsequent discharge to be produced by simultaneously applying both the sustain pulse (V_Y) of 190 V to the X electrode and the address pulse (V_Z) of 100 V to the address Z electrode.

Fig. 10 shows the schematics of the wall charges that accumulated on three electrodes during the discharge of mode 2. As shown in Fig. 10, the initial discharge in mode 2 is a plate gap discharge that is initiated between the Y–Z electrodes by simultaneously applying both the sustain pulse (V_X) of 190 V to the X electrode and the address pulse (V_Z) of 100 V to the Z electrode. During this trigger discharge, as shown in (i) of Fig. 10, many priming particles are produced within the discharge space, so that the particles with negative polarity, that is, the electrons, are transported toward the X electrode along the Z electrode applied by the positive voltage of 100 V. The resultant main discharge is produced, as shown in (ii) of Fig. 10. Finally, as shown in (iii) and (iv) of Fig. 10, the electrons accumulated on the X electrode, whereas the ions accumulated on both Y and Z electrodes. Fig. 11 shows the temporal IR profiles measured in two different discharge modes of cases (a) and (b). As mentioned above, the self-erasing discharge is observed in case (a). In addition, the IR profile in case (b) is more intensive than that in case (a). Consequently, the luminance in case (b) is higher than that in case (a) during the sustain period, as shown in Table II. However, the luminous efficiency in case (a) is higher than that in case (b) thanks to the self-erasing discharge.

C. Numerical Analysis

To investigate in detail the difference between two discharge modes during the sustain period, a numerical analysis using a 2-D fluid model [12], [13] was applied, including Poisson, continuity, and drift-diffusion equations.

Fig. 12 shows (b) the spatial wall charge distribution, (c) spatial electron density distribution, and (d) current flowing in the three electrodes during and after the sustain discharge in mode 1 (a) when applying the sustain voltage (V_X) of 300 V

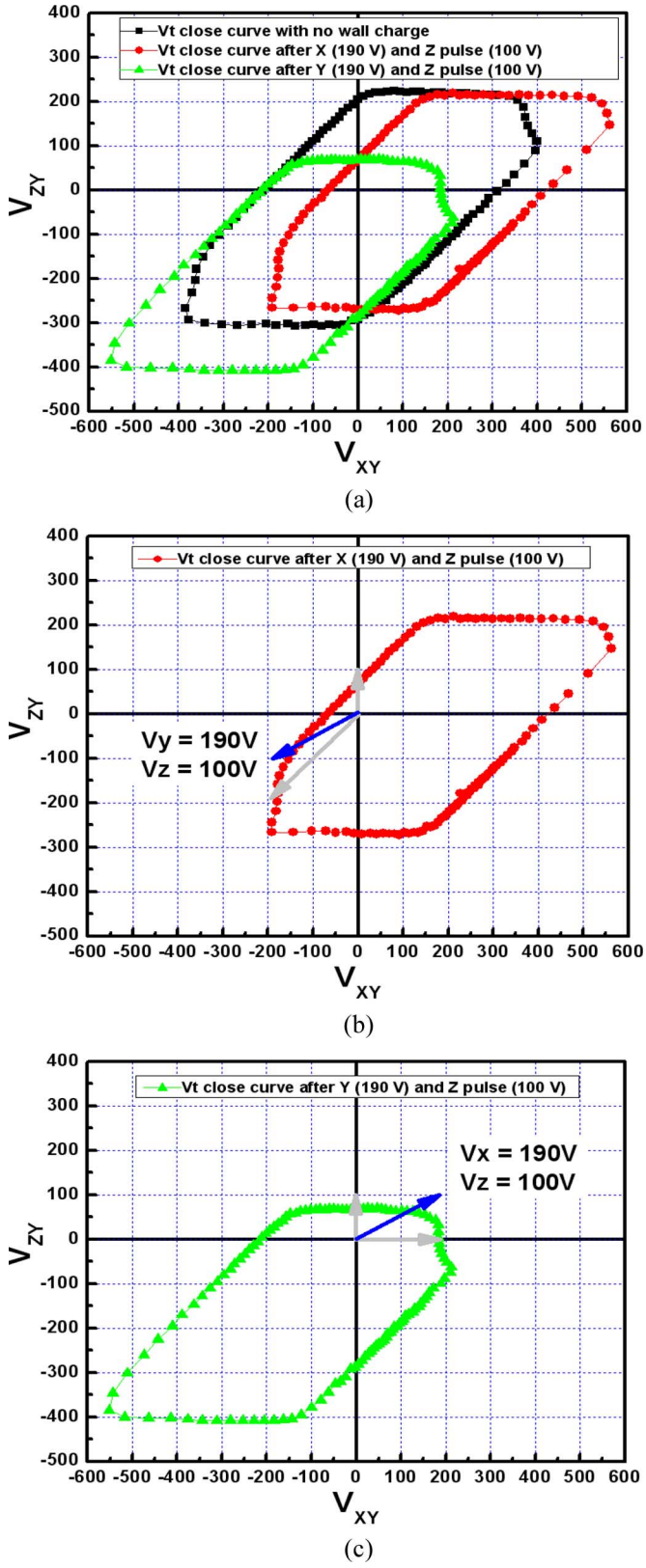

Fig. 9. (a) Shift of the V_t close curves measured after the sustain discharge is produced in discharge mode 2 with respect to the reference V_t close curve. (b) V_t close curve measured after applying both a sustain pulse V_X of 190 V to the X electrode and an address pulse V_Z of 100 V to the address Z electrode. (c) V_t close curve measured after applying both a sustain pulse VY of 190 V to the Y electrode and an address pulse V_Z of 100 V to the address Z electrode.

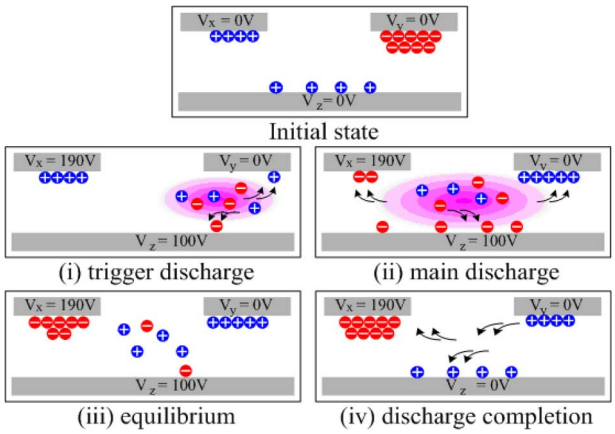

Fig. 10. Schematics of wall charges accumulating on three electrodes during discharges in mode 2.

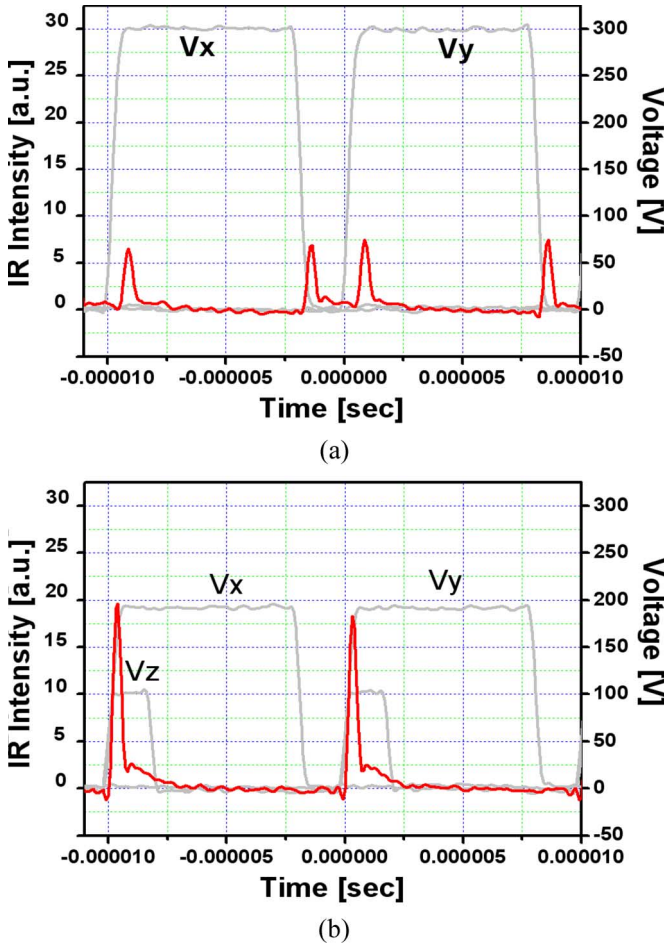

Fig. 11. Temporal IR profiles in two different discharge modes. (a) Mode 1. (b) Mode 2.

TABLE II
COMPARISON OF LUMINANCE AND LUMINOUS EFFICIENCY BETWEEN TWO DIFFERENT DISCHARGE MODES 1 AND 2

	Luminance [cd/m^2]	Luminous Efficiency [lm/W]
Case (a) (V_s: 300, V_z: 0 V)	830	1.34
Case (b) (V_s: 190, V_z: 100 V)	1008	1.26

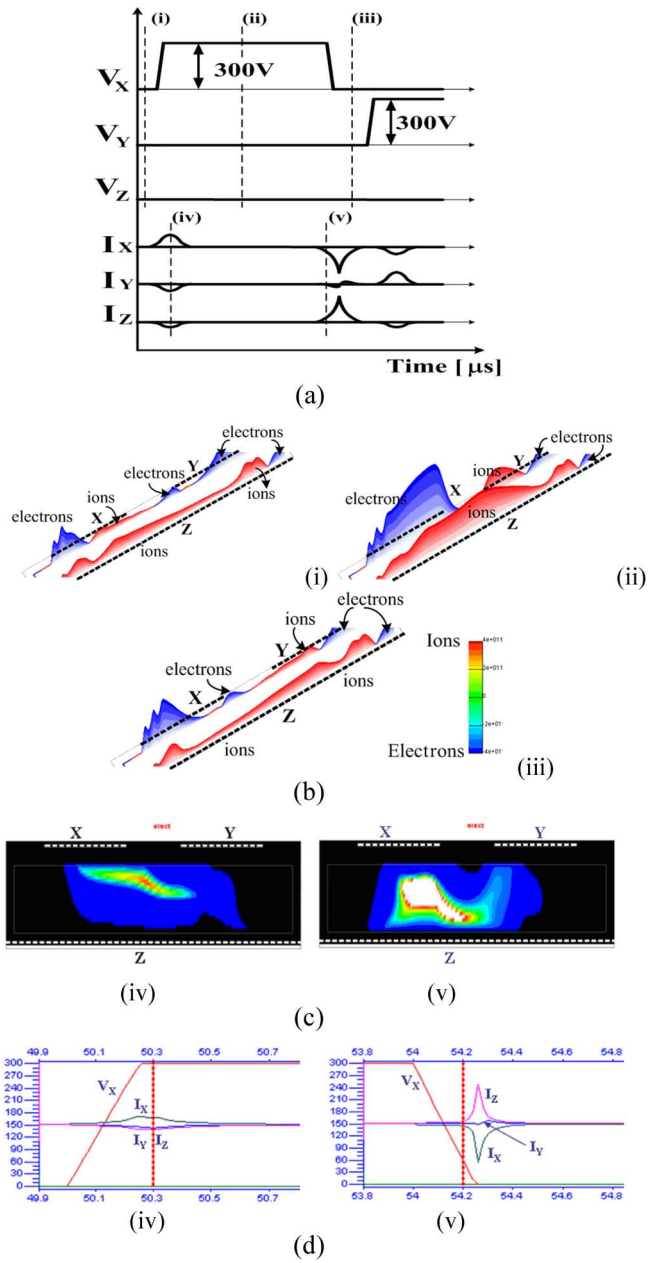

Fig. 12. (a) Voltage and current waveforms applied to three electrodes in mode 1. (b) Simulation results for spatial wall charge distributions (i, ii, and iii). (c) Spatial electron density distribution (iv and v). (d) Discharge current distributions (iv) during and (v) after sustain discharge.

to the X electrode. As shown in Fig. 12(b), the wall charges accumulating on the three electrodes prior to the main discharge (i) are considerably increased through the main discharge (ii) but are greatly decreased when the applied sustain pulse V_X decreases from 300 to 0 V (iii). This reduction of the wall charges is mainly due to the self-erasing discharge induced by the plate gap discharge between the X and Z electrodes, which is confirmed by the current data (v) in (d) of Fig. 12. Moreover, considering the trajectory of the electrons shown in Fig. 12(c), it is confirmed that the main discharge is produced between the X and Y electrodes, while the self-erasing discharge is produced between the X and Z electrodes.

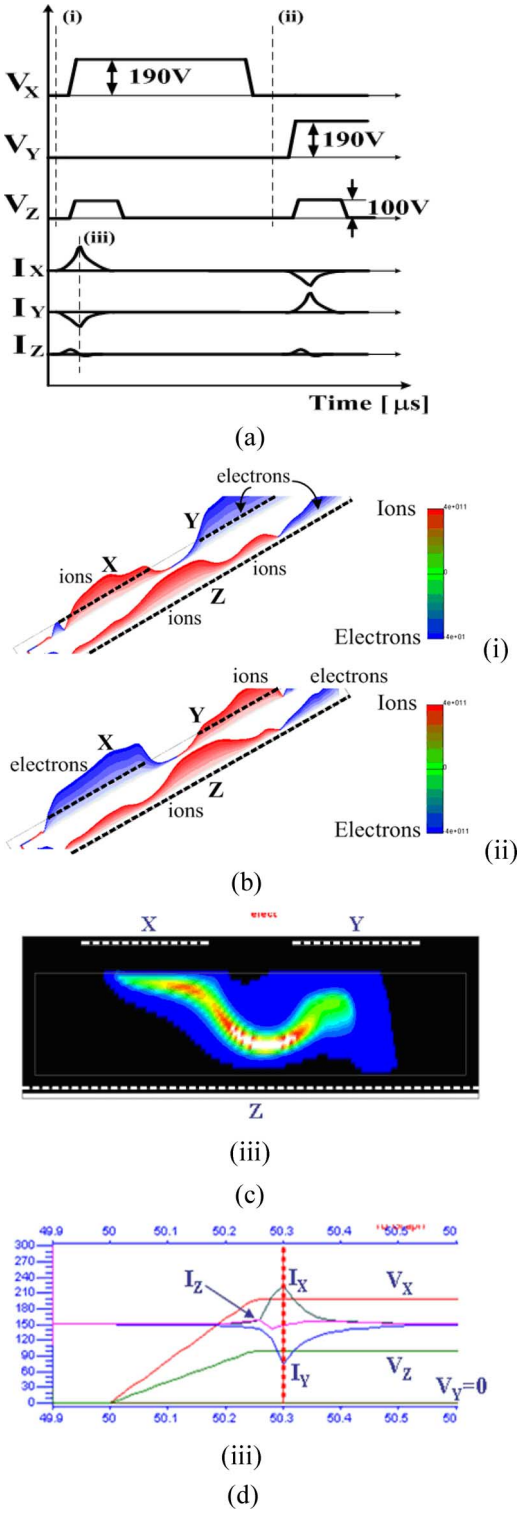

Fig. 13. (a) Voltage and current waveforms applied to three electrodes in mode 2. (b) Simulation results for spatial wall charge distributions (i and ii). (c) Spatial electron density distribution (iii). (d) Discharge current distributions during (iii) sustain discharge.

Fig. 13 shows the (b) spatial wall charge distribution, (c) spatial electron density distribution, and (d) current flowing in the three electrodes during the sustain discharge in mode 2 (a) when applying both the sustain voltage (V_X) of 190 V to the X electrode and the sustain voltage (V_Z) of 100 V to the Z electrode. Fig. 13(b) shows the wall charges accumulating on the three electrodes (i) prior to and (ii) after the main discharge, respectively. The discharge is produced once per sustain pulse, and the wall charges accumulating on the three electrodes after the main discharge are well distributed for the next sustain discharge. Fig. 13(c) and (d) shows the trajectory of the electron density and the discharge current flowing in the three electrodes during the sustain discharge in mode 2. As shown in Fig. 13(d), prior to the main X–Y discharge, the trigger discharge is initiated between the Y and Z electrodes, then extending toward the other X sustain electrode along the address electrode, and finally producing the main discharge. This sustain discharge in mode 2 is typically similar to that in a larger coplanar gap (> 400 μm) discharge. The numerical analysis confirms the different discharge characteristics, such as wall charge accumulations, electron density behavior, and current flowing in the three electrodes, for discharge modes 1 and 2.

IV. Conclusion

The discharge characteristics have been examined base on the variation in the voltage distribution among the three electrodes in the ac-PDP cell with a sustain gap of 200 μm. It has been observed that the two different discharge modes can be produced depending on the driving waveform. The two discharge modes have been examined and analyzed based on the V_t close-curve movement on the cell voltage plane. The two discharge modes show the different discharge characteristics, such as sustain voltage level, V_t close-curve behavior, luminance, and luminous efficiency. In addition, the spatial wall charge, electron density behaviors, and their current flows as a function of time have been investigated in detail using the numerical analysis.

References

[1] G. Oversluizen, M. Klein, S. de Zwart, S. van Heusden, and T. Dekker, "Discharge efficiency in plasma displays," *Appl. Phys. Lett.*, vol. 77, no. 7, pp. 948–950, Aug. 2000.

[2] J. D. Schemerhorn, E. Anderson, D. Levision, C. Hammon, J. S. Kim, B. Y. Park, J. H. Ryu, O. Shvydsky, and A. Sebastian, "A controlled lateral volume discharge for high luminous efficiency AC-PDP," in *Proc. SID*, 2000, pp. 106–109.

[3] L. F. Weber, "Positive Column AC Plasma Display," U.S. Patent 6184848 B1, Feb. 6, 2001.

[4] T. Callegari, J. Ouyang, N. Lebarq, B. Caillier, and J.-P. Boeuf, "3D modeling of a plasma display panel cell," in *Proc. Eurodisplay*, 2002, pp. 735–738.

[5] K. C. Choi, N. H. Shin, K. S. Lee, B. J. Shin, and S.-E. Lee, "Study of various coplanar gaps discharges in ac plasma display panel," *IEEE Trans. Plasma Sci.*, vol. 34, no. 4, pp. 385–389, Apr. 2006.

[6] H. Kim and H.-S. Tae, "Firing and sustaining discharge characteristics in alternating current microdischarge cell with three electrodes," *IEEE Trans. Plasma Sci.*, vol. 32, no. 2, pp. 488–492, Apr. 2004.

[7] J. Y. Kim, H. Kim, H.-S. Tae, J. H. Seo, and S.-H. Lee, "Effects of voltage distribution among three electrodes on microdischarge characteristics in ac-PDP with long discharge path," *IEEE Trans. Plasma Sci.*, vol. 34, no. 6, pp. 2579–2587, Dec. 2006.

[8] H.-S. Tae, S.-K. Jang, K.-D. Cho, and K.-H. Park, "High-speed driving method using bipolar scan waveform in AC plasma display panel," *IEEE Trans. Electron Devices*, vol. 53, no. 2, pp. 196–204, Feb. 2006.

[9] K. Sakita, K. Takayama, K. Awamoto, and Y. Hashimoto, "High-speed address driving waveform analysis using wall voltage transfer function for three terminals and V_t close curve in three-electrodes surface-discharge AC-PDPs," in *Proc. SID*, 2001, pp. 1022–1025.

[10] H. J. Kim, J. H. Jeong, K. D. Kang, J. H. Seo, I. H. Son, K. W. Whang, and C. B. Park, "Voltage domain analysis and wall voltage measurement for surface-discharge type ac-PDP," in *Proc. SID*, 2001, pp. 1026–1029.
[11] H. Inoue, Y. Seo, K. Sakita, and Y. Hashimoto, "Numerical analysis of V_t close curve for non-uniform wall charge distribution in three-electrode AC-PDP," in *Proc. Eurodisplay*, 2002, pp. 931–934.
[12] S.-B. Song, P.-Y. Park, H.-Y. Lee, J.-H. Seo, and K. D. Kang, "Stability of weak discharge at Y-reset period in plasma display panel discharge," *Surf. Coat. Technol.*, pp. 140–143, 2002.
[13] J. H. Seo, W. J. Chung, C. K. Yoon, J. K. Kim, and K. W. Whang, "Two dimensional modeling of a surface type alternating current plasma display panel cell: Discharge dynamics and address voltage effects," *IEEE Trans. Plasma Sci.*, vol. 29, no. 5, pp. 824–831, Oct. 2001.

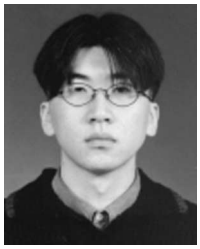

Jae Young Kim received the B.S. and M.S. degrees in electronic and electrical engineering in 2002 and 2004, respectively, from Kyungpook National University, Daegu, Korea, where he is currently working toward the Ph.D. degree in electronic engineering.

His current research interests include high-pressure plasma and microdischarge physics for plasma display applications.

Heung-Sik Tae (M'00–SM'05) received the B.S., M.S., and Ph.D. degrees from Seoul National University, Seoul, Korea, in 1986, 1988, and 1994, respectively, all in electrical engineering.

Since 1995, he has been a Professor with the School of Electrical Engineering and Computer Science, Kyungpook National University, Daegu, Korea. His research interests include the optical characterization and driving circuit of plasma display panels (PDPs), the design of millimeter-wave guiding structures, and electromagnetic wave propagation using meta-material.

Dr. Tae is a member of the Society for Information Display. He has been serving as Editor for the IEEE TRANSACTIONS ON ELECTRON DEVICES, section on flat panel display, since 2005.